Available online at www.sciencedirect.com

ScienceDirect

Journal of Hydro-environment Research 9 (2015) 187–199

Journal of Hydro-environment Research

www.elsevier.com/locate/jher

Research paper

Integrated water quality modelling: Application to the Ribble Basin, U.K.

Brian A. Boye [a,*], Roger A. Falconer [b], Kunle Akande [c]

[a] Hydro-environmental Research Centre, Cardiff School of Engineering, Cardiff University, The Parade, Cardiff CF24 3AA, United Kingdom
[b] CH2M HILL, Hydro-environmental Research Centre, Cardiff School of Engineering, Cardiff University, The Parade, Cardiff CF24 3AA, United Kingdom
[c] CH2M HILL, Burderop Park, Swindon, Wiltshire SN4 0QD, United Kingdom

Available online 18 September 2014

Abstract

This paper reviews the traditional approach of linking models to cover integrated water management from the upper reaches of catchments through river basins, into estuaries and to the coastal/marine environment. It highlights some of the deficiencies in the approaches currently being adopted in many non-integrated studies, where artificial boundaries are included in the system, and then highlights the need for a more integrated conceptual approach. A case study is discussed, namely the non-compliance of bathing waters along the Fylde Coast and Ribble Basin (U.K.) from riverine inputs, with the inputs arising from Waste water Treatment Works (WwTW), outfalls and drainage systems. A more integrated approach was applied to this estuary, with refinements to the artificial boundaries. Both hydrodynamic and solute transport processes in 1-D and 2-D domains of this estuary were modelled for a wet event in June 1999. The bio-kinetic decay process representation included the impacts of salinity, solar irradiation, turbidity and water temperature on the decay rate. Solutes modelled included faecal coliform, water temperature and salinity. This paper demonstrates that a similar or better accuracy of the coliform concentrations can be achieved using an integrated model based on a realistic representation of physical and biochemical processes. This is significant because the integrated model does not need extensive calibration to give good results. This is therefore a much more robust model which is not influenced significantly by the position of boundaries. The robustness of the model gives increased confidence in predicted results for new scenarios where measured data is not available. This is particularly important for all types of real time water quality prediction (e.g. toxic spills) including bathing water quality. Hence better decisions can be made when considering investment strategies, appropriate for various treatment options and catchment management solutions in the river basin upstream.

Keywords: Water quality; Coliform bacteria; Temperature; Salinity; Solar irradiation; Computational modelling

1. Introduction

In the current environment where nations are increasingly accepting that climate change is occurring and more countries are experiencing the impact of climate change, through increased floods, more intense storms or more droughts etc., there is a growing interest world-wide in adopting a more integrated approach to river basin management, particularly when rivers cross states and countries. Bathing water quality is an important public health issue, mainly because of faecal contamination (Mansilha et al., 2009). There is considerable epidemiological evidence in the literature to suggest that contact with polluted recreational water is a risk factor for gastrointestinal illness, including serious health problems such as infection with Shigella Sonneri, Escherichia Coli O157, protozoan parasites and enteric viruses, mainly derived from human sewage or animal sources (Prüss, 1998; Pond, 2005; Nicholis, 2006; Schets et al., 2011). Epidemiological studies have used bathing trials to examine the relationship between microbiological indicators of water quality and diaries of symptoms kept by the participating volunteers (Kay et al., 1994). The European Union (EU) have published the Bathing Water Directive (European Parliament, 2006), where in

* Corresponding author. Tel.: +44 7865076893.
E-mail addresses: boyeba1@cf.ac.uk, brian.boye@brinsy.com (B.A. Boye), FalconerRA@cf.ac.uk (R.A. Falconer), kunle.akande@ch2m.com (K. Akande).

http://dx.doi.org/10.1016/j.jher.2014.07.002

member states are required to set up river basin management plans. Within this Directive, EU Member States are required to manage both point and diffuse sources of pollution to achieve 'good' ecological status and water quality by 2015 (European Parliament, 2006; Kay et al., 2008).

Integrated water management is not new; many research teams and companies have been modelling the system from the Cloud to Coast (C2C) for a number of years, but in many of these instances there have been different teams or individuals working on modelling and monitoring the catchment, river, estuary and coastal basins and, all too often, using different parameters and formulations for various processes within each sub-set of the system as a whole. When models are linked from catchments to rivers, and particularly rivers to estuaries and coastal basins, artificial boundaries are created in a natural system where, in general, no such boundary exists in nature. When the raindrop falls from the cloud to the catchment and moves from the stream to the river, to the estuary and to the sea/coast, it does not know at any stage whether it is in the river or in the estuary as depicted in Fig. 1.

It is the modeller who creates the artificial boundary and we need to ensure that such boundaries are as smooth and as transparent as possible. For example, it is imperative that when a 1-D model is linked to a 2-D model there should not be a sudden change in the bed friction or in diffusion/dispersion values included in the integrated model unless the sudden change can be technically justified. Thus the challenge is to have a truly integrated water management system for accurate and effective solutions and this paper seeks to develop appropriate solution methods for the implementation of a Cloud to Coast (C2C) solutions approach. Real-time water quality predictions are becoming more important globally, from Western Europe to East Asia (Thoe et al., 2012; Chan et al., 2013) as more laws are introduced by Governments to control water quality for all types of environmental problems from toxic spills to bathing waters. Having an integrated model where the results are not affected by the position of artificial boundaries will be highly beneficial to industry (Boye et al., 2013).

2. Integrated modelling details

In applying the C2C conceptual approach to practical river and coastal basin studies, involving environmental and eco-hydraulics problems, details are first given herein of the integrated modelling formulations used to simulate the hydrodynamic and solute transport processes in river and coastal systems. The flow and solute inputs from the catchments are not included in these equations, but were provided from the use of field data and land-use management models as outlined later in the paper.

The hydro-environmental models used by river and coastal engineers and environmental managers to predict the hydrodynamic, water quality and sediment transport processes in river and coastal systems are based on first solving the governing hydrodynamic and solute transport equations. For a Cartesian co-ordinate system, with the main body of the flow in the x-direction and being assumed to be incompressible and inviscid, the corresponding 1-D St Venant equations for mass and momentum conservation can be written as:

$$\frac{\partial A}{\partial t} + \frac{\partial Q}{\partial x} = 0 \tag{1}$$

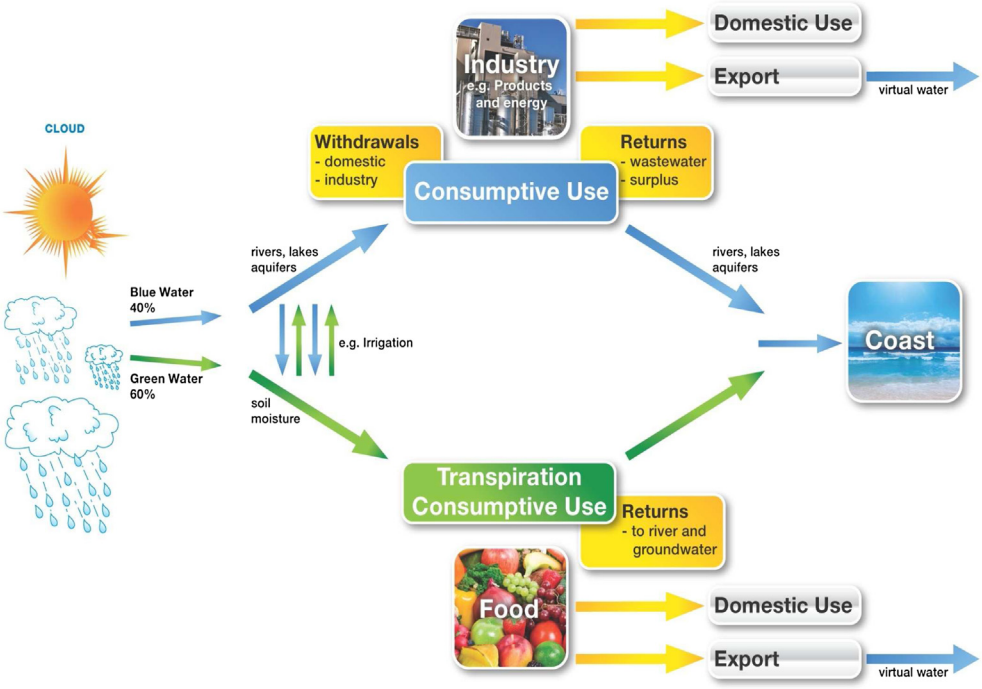

Fig. 1. The water cycle (The Royal Academy of Engineering (2010)).

$$\frac{\partial Q}{\partial t}+\underbrace{\beta_1\frac{2Q}{A}\frac{\partial Q}{\partial x}-\beta_1\frac{Q^2}{A^2}\frac{\partial A}{\partial x}}_{\text{advection}}=\underbrace{-gA\frac{\partial \eta}{\partial x}}_{\text{pressure}}-\underbrace{g\frac{Q|Q|}{C^2AR}}_{\text{friction}} \tag{2}$$

where Q is the flow rate, η is the surface water elevation, A is the cross-sectional area of flow, β_1 is the momentum correction factor (assumed to be 1.06 for a seventh power law velocity profile in this study), g is the acceleration due to gravity, R is the hydraulic radius and C is the Chezy roughness coefficient (evaluated from a Nikuradse roughness coefficient in this study). Equation (1) describes the conservation of mass while Equation (2) describes the conservation of momentum for a 1-D flow. The one-dimensional equations are suitable for hydrodynamic problems where the vertical and lateral velocity components are small in comparison with the stream wise velocity component (e.g. river flows).

For two-dimensional flow, the Reynolds Averaged Navier–Stokes equations for mass and momentum conservation can be written as:

$$\frac{\partial \eta}{\partial t}+\frac{\partial q_x}{\partial x}+\frac{\partial q_y}{\partial y}=0 \tag{3}$$

$$\begin{aligned}\frac{\partial q_x}{\partial t}&+\underbrace{\beta_2\left(\frac{2q_x}{H}\frac{\partial q_x}{\partial x}-\frac{q_x^2}{H^2}\frac{\partial H}{\partial x}\right)+\beta_2\left(\frac{q_x}{H}\frac{\partial q_y}{\partial y}+\frac{q_y}{H}\frac{\partial q_x}{\partial y}-\frac{q_xq_y}{H^2}\frac{\partial H}{\partial y}\right)}_{\text{advective acceleration}}\\&=\underbrace{-gH\frac{\partial \eta}{\partial x}}_{\text{pressure}}+\underbrace{2\frac{\partial}{\partial x}\left[\varepsilon_t H\frac{\partial \overline{u}}{\partial x}\right]+\frac{\partial}{\partial y}\left[\varepsilon_t H\left(\frac{\partial \overline{u}}{\partial y}+\frac{\partial \overline{v}}{\partial x}\right)\right]}_{\text{turbulent / eddy stress}}\\&\quad-\underbrace{\frac{gq_x\sqrt{q_x^2+q_y^2}}{H^2C^2}}_{\text{bed stress}}\end{aligned} \tag{4}$$

$$\begin{aligned}\frac{\partial q_y}{\partial t}&+\underbrace{\beta_2\left(\frac{q_x}{H}\frac{\partial q_y}{\partial x}+\frac{q_y}{H}\frac{\partial q_x}{\partial x}-\frac{q_xq_y}{H^2}\frac{\partial H}{\partial x}\right)+\beta_2\left(\frac{2q_y}{H}\frac{\partial q_y}{\partial y}-\frac{q_y^2}{H^2}\frac{\partial H}{\partial y}\right)}_{\text{advective acceleration}}\\&=\underbrace{-gH\frac{\partial \eta}{\partial y}}_{\text{pressure}}+\underbrace{2\frac{\partial}{\partial x}\left[\varepsilon_t H\frac{\partial \overline{v}}{\partial x}\right]+\frac{\partial}{\partial y}\left[\varepsilon_t H\left(\frac{\partial \overline{v}}{\partial y}+\frac{\partial \overline{u}}{\partial x}\right)\right]}_{\text{turbulent / eddy stress}}\\&\quad-\underbrace{\frac{gq_y\sqrt{q_x^2+q_y^2}}{H^2C^2}}_{\text{bed friction}}\end{aligned} \tag{5}$$

where H is the flow depth, q_x, q_y are the depth integrated velocities (mean velocity times flow depth) in the x and y directions respectively, $\overline{u}$, $\overline{v}$ are the time averaged velocities in the x and y directions respectively, β_2 is the momentum correction coefficient (assumed to be 1.016 as before), and ε_t is the turbulent eddy viscosity. The parabolic eddy viscosity turbulence model is adopted in this study and hence the eddy viscosity is given as $\varepsilon_t = \alpha_1 U^* H$ where, for this study, α_1 is assumed to be 1.0, based on calibration with field data.

The solute transport equations for 1-D and 2-D flow can be described as:

$$\frac{\partial AS}{\partial t}+\underbrace{\frac{\partial AUS}{\partial x}}_{\text{advection}}-\underbrace{\frac{\partial}{\partial x}\left[A(D_{tx}+D_{Lx})\frac{\partial S}{\partial x}\right]}_{\text{diffusion / dispersion}}=\underbrace{-k_b'SA}_{\text{decay}} \tag{6}$$

$$\begin{aligned}&\frac{\partial HS}{\partial t}+\underbrace{\frac{\partial HUS}{\partial x}+\frac{\partial HVS}{\partial y}}_{\text{advection}}\\&\quad\underbrace{-\frac{\partial}{\partial x}\left[H(D_{tx}+D_{Lx})\frac{\partial S}{\partial x}\right]-\frac{\partial}{\partial y}\left[H\left(D_{ty}+D_{Ly}\right)\frac{\partial S}{\partial y}\right]}_{\text{diffusion / dispersion}}\\&\quad=\underbrace{-k_b'SH}_{\text{decay}}\end{aligned} \tag{7}$$

where S is the mean solute concentration (i.e. area averaged for 1-D and depth averaged for 2-D), U, V are the mean velocities in the x and y directions respectively, D_{tx} is the turbulent diffusion coefficient, D_{Lx} is the longitudinal dispersion coefficient, k_b' is the first order effective decay rate and H is the depth of flow. Equations (6) and (7) describe the 1-D and 2-D solute mass conservation equations respectively. The longitudinal dispersion coefficient, D_{Lx}, is a function of the shear velocity, U^* and the flow depth, H, and, according to Elder (1959) is given as:

$$D_{Lx}=k_l U^* H \tag{8}$$

where k_l is a constant of proportionality.

In modelling water quality processes in rivers and coastal basins a range of indicator organisms are often modelled as outlined in Falconer and Chen (1996). However, in this research study the main biological indicator of water quality considered was faecal coliform, which is measured by the number of colony forming units (cfu). Bacteria are modelled as solutes (Equation (7)), with a source term that assumes a first order decay of the solute and includes input sources such as outfalls. The expression (Equation (9)) used for the decay rate of bacteria includes the effects of: water temperature, solar irradiation, turbidity, salinity and temperature. This expression is a modified version of that given by Chapra (2008), with the added assumption that the effects of solar irradiation are dependent on water temperature, giving:

$$k_b'=(k_b+k_i+k_{\text{sal}})\theta_w^{T-20^\circ C} \tag{9}$$

where k_b' = effective total decay rate (per day), k_b = base mortality rate in fresh water at 20 °C under dark conditions, k_{sal} = mortality rate due to salinity, θ_w = empirical coefficient for water temperature effects and T = water temperature. The decay rate due to solar irradiation is given as:

$$k_i = \alpha_i I_o(t) \frac{1.0 - e^{-k_e H}}{k_e H} \quad (10)$$

where α_i = coefficient of irradiation which is dependent on the type of bacteria, $I_o(t)$ = intensity of solar irradiation and k_e = extinction coefficient of light. The decay rate due to salinity is given as:

$$k_{\text{sal}} = \theta_s C_{\text{sal}} \quad (11)$$

where θ_s = coefficient of salinity and C_{sal} = salinity.

3. Integrated model application to the Ribble Basin

3.1. General

The Ribble estuary and river basin is located along the north-west coast of England. Until the late 1970s the main channel of the estuary, which is enclosed within a training wall, was regularly dredged to allow passage to the upper estuary for shipping (Lyons, 1997). At the mouth of the estuary, there are two well known seaside resorts, namely Lytham St Annes and Southport, with both being designated EU (European Union) Bathing Waters. The Fylde Coast, which is bounded between Fleetwood to the north and the Ribble estuary to the south, includes one of the most famous beaches for tourism in England, namely Blackpool, with an average of more than 17 million visitors per annum. The area has four main centres of population, namely: Blackpool and Lytham St Annes to the north of the Ribble estuary, Southport to the south of the estuary, and the town of Preston, which is inland and straddles the river Ribble at the tidal limit (Fig. 2).

In order to enhance the bathing water quality along the Flyde coast, a major civil engineering investment programme was undertaken in recent years to reduce the bacterial input to the estuary. Over $800 million has been invested over the past 20 years in new sewerage treatment plants and water treatment works along the Fylde Coast and Ribble estuary. Examples include:- upgrading the Waste water Treatment Works (WwTW) at Clifton Marsh from primary treatment to include UV disinfection; and reducing storm water discharges from the waste water network by constructing 260,000 m^3 of additional storage. Recently, a major capital works project (approximately $250 million) was undertaken by United Utilities, to enhance the sewer system in Preston, and with the aim of reducing the pollution discharges to the river Ribble (United Utilities, 2013). The project was completed in March 2014. The project is split into two sub projects which are called Preston Tunnel and Preston 32. Although the reduction in input bacterial loads has resulted in a marked decrease in the concentration of bacterial indicators in the coastal receiving waters, occasional elevated faecal coliform counts have still been measured at the compliance points (Crowther et al., 2001). As a result, the bathing waters have still occasionally failed to comply with the EU mandatory water quality standards of the Bathing Water Directive. There has also been work carried out to try to establish links between sources of bacterial indicators and the quality of the coastal waters. For example, Kay et al. (2005b) investigated the relationship between land use and faecal indicator organism concentrations and concluded that built-up areas with their associated related sewage inputs were a significant source of faecal indicator organisms in the Ribble drainage basin. In this paper a deterministic model is used to predict the faecal coliform levels. However, other methods can also be used, as well as being linked to deterministic hydro-environmental models. For example, Kashefipour et al. (2005) applied an Artificial Neural Network (ANN) model in order to predict faecal coliform concentration levels at compliance points along bathing water zones situated in the south west of Scotland, U.K. However, the deterministic nature of computational fluid dynamics models generally makes them more accurate in predicting coliform levels and particularly for possible future scenarios with related investment strategies.

3.2. Previous integrated model application

A hydro-environmental modelling study was originally undertaken to establish the water quality of the EU designated bathing waters located near the mouth of the Ribble estuary (Kashefipour et al., 2002). The previous study assessed the effectiveness of a range of strategic options, including: the effects of adding UV treatment, constructing storm water storage tanks and incorporating various combined storm water overflow (CSO) discharge scenarios for different weather conditions. In order to reduce the possible inaccuracies caused by setting up the boundary conditions required to drive the numerical models, the upstream boundaries were located at the tidal limits of the rivers Ribble, Darwen and Douglas (see Fig. 2) and the downstream boundary was located around the 25 m depth contour in the Irish Sea. The length of the seaward boundary was 41.2 km, with the width of the upstream river boundaries being generally less than 10 m. Such a great variation in the modelling dimensions made it impractical to use either a 1-D or 2-D model alone. In applying either of these two models individually, or linking the models statically, would have introduced inaccuracies in the model prediction results and would also have required a considerable amount of effort in exchanging the data. Thus, in this study a 1-D and 2-D model (namely FASTER and DIVAST) were linked dynamically (i.e. exchanging data over the linked boundary at each time step with the width of the boundary varying due to the processes of wetting and drying) to create a single model, in which the numerical simulations of the hydrodynamic variables and bacterial indicators were undertaken simultaneously across the entire modelling region.

3.3. C2C refinements on bathing water quality in the basin

3.3.1. Review of original study

In reviewing the original study of Kashefipour et al. (2002), in the context of a C2C solutions approach, the authors found a

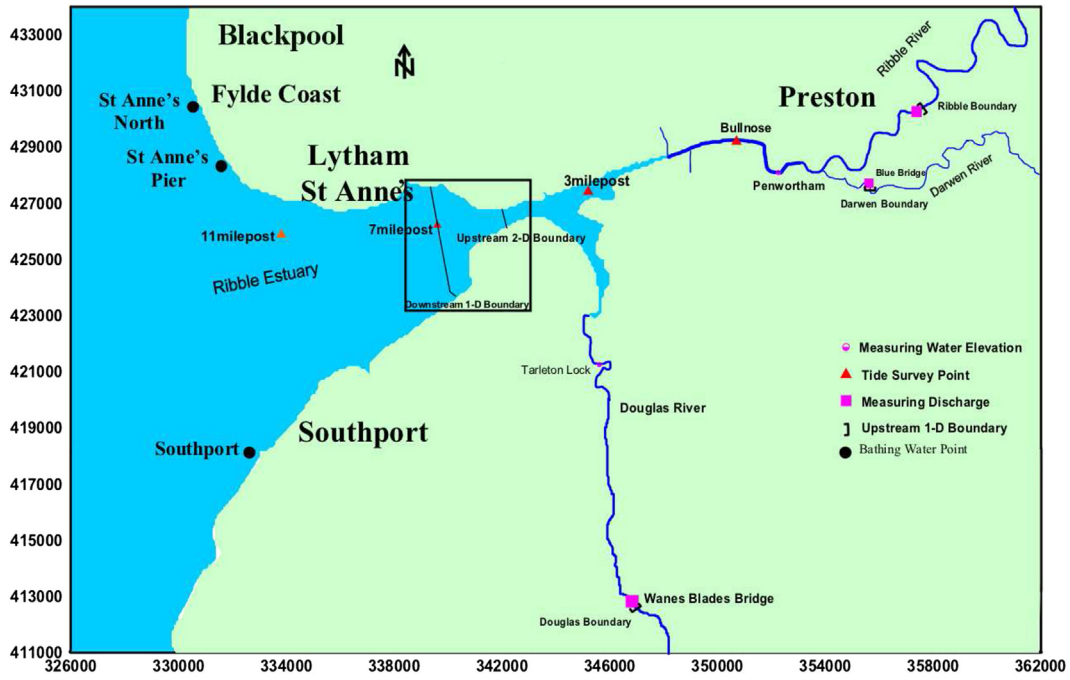

Fig. 2. Fylde Coast, showing the Ribble estuary and its tributaries (Grid in metres).

number of anomalies with the original study and some key lessons learnt for the future, particularly in the context of the principle that the raindrop, possibly with a pollutant attached (either in solution or in particulate form if linked to a sediment particle), does not know whether it is in a catchment stream, river, estuary or coastal basin. Taking account of these anomalies the following observations were made with regard to the original studies:

1. Different values of the decay rate were used in the 1-D and 2-D domains of the linked model (see Table 1), with the decay rate being higher in the 2-D domain of the linked model in comparison with the 1-D domain; there was no physical or biochemical justification for this change;
2. Different values and formulations of the dispersion coefficient were used in the 1-D and 2-D domains of the linked model (Fig. 3). An empirical formulation for rivers was used in the 1-D domain (Kashefipour and Falconer, 2002) whilst in the 2-D domain the formulation by Preston (1985) was used;
3. Different values and formulations were used for the bed friction term in the 1-D and 2-D equations, with the Manning equation being used in the 1-D domain and with the Colebrooke-White and the Nikuradse equivalent sand grain roughness 2-D domain, when there was no physical reason for this change;
4. The same water temperature of 14 °C was used in both the 1-D and 2-D domains of the dynamically linked model;
5. The effects of salinity on the decay rate were not explicitly defined;
6. The effects of solar irradiation were considered in a step change manner from night to day in the decay rate; and
7. There was a large overlap area, linking the 1-D and 2-D domains of the linked model.

Table 1
Faecal coliform decay rates for old model.

		1-D domain		2-D domain	
		$k_b + k_i$	(k'_b)	$k_b + k_i$	(k'_b)
Day	Decay rate (/day)	0.85	(0.645)	1.0	(0.759)
	T_{90} value (hr)	65.0	(85.7)	55.3	(72.8)
Night	Decay rate (/day)	0.5	(0.379)	0.68	(0.516)
	T_{90} value (hr)	110.5	(145.8)	81.3	(107.1)

In adopting a C2C solutions approach to this study site, the integrated Cloud to Coast (C2C) model was re-run using the same formulations for the momentum correction coefficient, turbulent eddy viscosity, Manning roughness coefficient, dispersion and diffusion coefficients and the kinetic decay rates along the whole river and coastal basin and with the

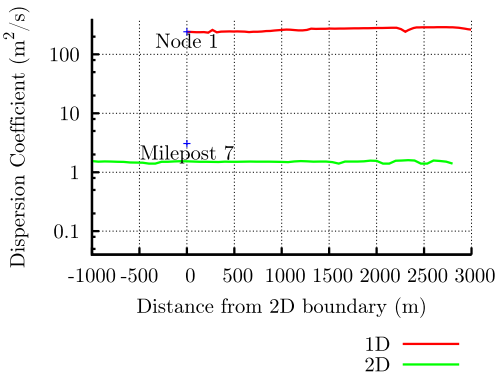

Fig. 3. Dispersion coefficients in both 1-D and 2-D model domains at 30 h.

various parameters only being changed where there were sound technical reasons for doing so. This differed from the previous study where the value of the parameter was very much based on whether the 'water package' was in the 1-D or 2-D model domain.

In the following sections, differing parameters are introduced into the numerical model developed for this research study, starting with input parameters similar to those used by Kashefipour (2002). Finally, the effects of all of the input parameters are considered simultaneously. A summary of these input parameters is given in Table 2.

For each set of parameters in Table 2 the measured and predicted coliform concentrations were compared qualitatively and quantitatively. A quantitative comparison was undertaken by calculating the mean absolute error (MAE) for the $\log_{10}$ transformed concentrations at three survey points, namely: Milepost 7, Milepost 3 and Bullnose (see Fig. 2).

3.3.2. Common decay rates

In the revised model, the T_{90} value was set at 20 h for daytime and 100 h for night time in both the 1-D and 2-D models. The equivalent daytime decay rate (i.e 2.76 per day) was therefore higher than the values in the previous 'old' model (Kashefipour et al., 2002). The equivalent night time decay rate (i.e. 0.55 per day) was lower than that in the 2-D part of the old model.

A comparison of the resulting faecal coliform predictions is shown in Fig. 4, both for the old and new models.

The results of this comparison show that whilst the old model, which was calibrated for the best results for each reach, gave the best agreement (i.e. MAE of 0.235) for the peak faecal coliform levels as compared to the revised model (i.e. MAE of 0.348), there is no doubt that the revised model was more representative of the actual biochemical decay processes. In particular, the more holistic model was more robust for predicting the impacts of changes to the systems, such as climate change, new WwTWs discharge levels etc.

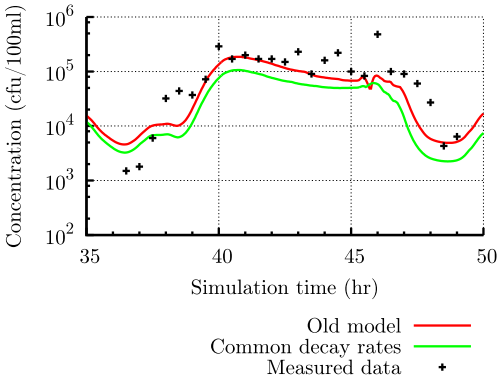

Fig. 4. Faecal coliform levels with time for the new (common decay rates) and old model after introduction of common decay rates.

3.3.3. Refinement of linked boundary

In the old model of Kashefipour (2002), the length of the linking overlap reach between the 1-D and 2-D models was about 2.8 km long (Fig. 5(a)). This overlap length is relatively large compared to the grid size (66.67 m × 66.67 m) in the 2-D model and the distance between cross-sections of 10 m–50 m in the 1-D model. The linear nature of the variation of minimum bed elevation with distance for the 1-D domain of the model, shown in Fig. 5(a), shows that the cross-sections must have been generated using linear interpolation. This is confirmed in the thesis of Kashefipour (2002).

Table 2
Summary of parameters used in revised analysis and resulting MAE values.

	Old Model	Common Decay Rates	Common Dispersion	Improved Link	Common Friction	Water Temperature	Salinity	Solar Irradiation	Turbidity	Combined Effects
Night value k_b = 0.553/day (T_{90}=100 hr), Maximum Day value $k_b + k_i$ = 2.763/day (T_{90}=20 hr)		•	•	•	•	•	•	•	•	•
Use of the same dispersion formulation in both domains with k_l=90			•	•	•	•	•	•	•	•
Removal of linked boundary overlap				•	•	•	•	•	•	•
Use of Manning's n in both domains and gradual linear variation over linked boundary					•	•	•	•	•	•
18 °C at upstream boundary of 1-D domain, 14 °C at downstream boundary of 2-D domain and water temperature coefficient θ_w=1.047						•				•
0.5 ppt at upstream boundary of 1-D domain, 35 ppt at downstream boundary of 2-D domain and salinity coefficient θ_s=0.02 day^{-1} ppt^{-1}							•			•
Sinusoidal variation of irradiation with maximum of 900 W m^{-2}, day length = 12 hours and irradiation coefficient α= 2.456 day^{-1} m^2 kW^{-1}								•		•
Turbidity in the form of light extinction coefficient k_e=2.37 m^{-1}									•	•
Mean Absolute Error (MAE) of $\log_{10}$ transformed concentrations at three survey points	0.235	0.348	0.333	0.276	0.272	0.294	0.270	0.236	0.196	0.203

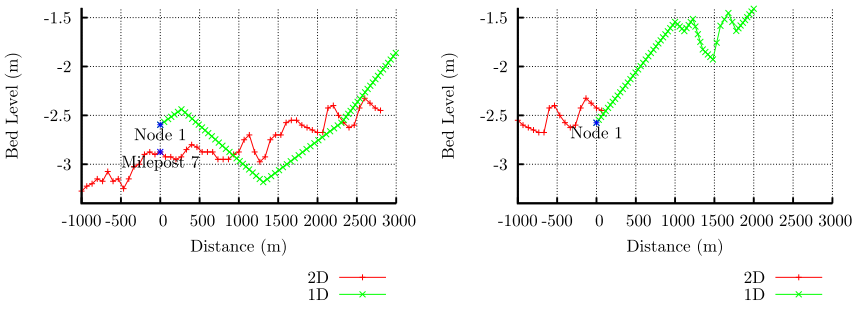

Fig. 5. Longitudinal section through link overlap area.

There are several ways of linking or coupling models. One approach is to use a simpler (1-D) model over the entire solution domain and a more complex (2-D) model in confined sub-domains (Wu, 2008). For this case the simpler model provides boundary conditions for the more complex model, but they are not fully coupled. This approach is called hybrid modelling. Another approach is to fully couple the models by simultaneously solving all component models. Overlapping and non-overlapping interfaces can be used to couple the models (Wu, 2008). The disadvantage of overlapping interfaces is that a region with two sets of differing formulations and results (e.g. velocities and water elevations) is created. The difference between the velocities in this region can introduce uncertainty into the overall model. In a water quality model, the solute transport in the same overlapped region will be dependent on two sets of velocities. This is inconsistent, as the same solute cannot have two different velocities at the same location. The overlap is usually present to ensure numerical stability between the two domains, however, this can lead to an inconsistent solution in terms of accuracy, between the two domains (Zhou et al., 2014). In this study, at the interface between the 1-D and 2-D models, velocities, water elevations and solute concentrations are all exchanged after each time-step (Fig. 6).

To improve on the accuracy over the linked boundary, the area of the linked overlap was reduced. This was done by truncating the length of the 1-D domain until the number overlapping grid cells in the 2D domain was reduced to just one (Fig. 7). The data exchange at the overlap was also modified so that instead of transferring data from just one cell in the 2-D domain, an average over the wet cells at the linked interface was used as shown in Fig. 7.

The revised geometry at the linked boundary is shown in Fig. 5. As a result of the changes to the linked boundary configuration, the conservation of mass and momentum across the boundary was significantly improved. The resulting effects on the coliform concentration predictions led to a reduction in the MAE over the three survey points to 0.276 (see Fig. 8 and Table 2) which was greater than that of the old model (i.e. MAE of 0.235). Compared to the model without modifications at the linked boundary the changes in the predictions are small, however, the improved boundary representation enhanced the overall integrated model behaviour under varying conditions and its robustness for new scenarios. As shown in Fig. 8, the improved linked boundary led to higher concentrations of faecal coliform travelling further downstream.

3.3.4. Common bed friction

Different values and formulations were used in the old model for the bed friction term, in the 1-D domain (i.e. Manning's $n = 0.021$) and with the Nikuradse equivalent sand grain roughness being used in the 2-D domain ($k_s = 20$ mm, equating to a Manning's n value of approximately 0.208), with the Colebrook-White equation being solved for in the dynamically linked model. Again, there was no physical reason why the values of the frictional resistance should change between the 1-D and 2-D domains. This was the result of the domains being calibrated independently in the previous study. In the refined new model, the value of Manning's n was varied linearly over the first reach so that the bed friction varied gradually over the linked boundary. In addition, the Manning equation was used to calculate the bed friction in both the 1-D and 2-D domains of the linked model. The resulting water elevations, current speeds and faecal coliform levels due to the revised variation of Manning's n close to the linked boundary were not significantly different (i.e a

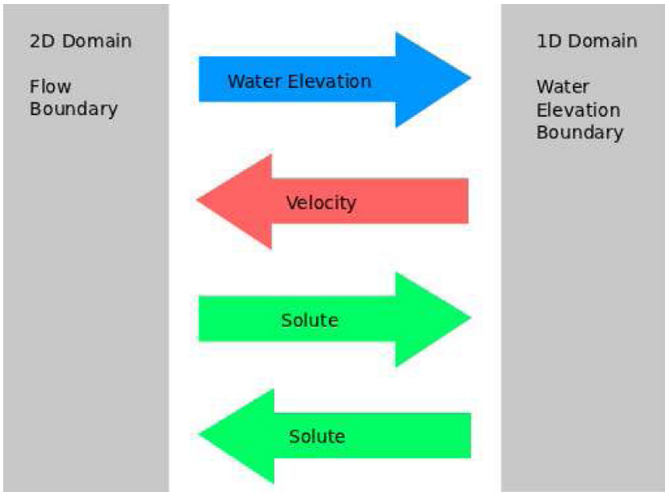

Fig. 6. Exchange of data across 1D-2D link.

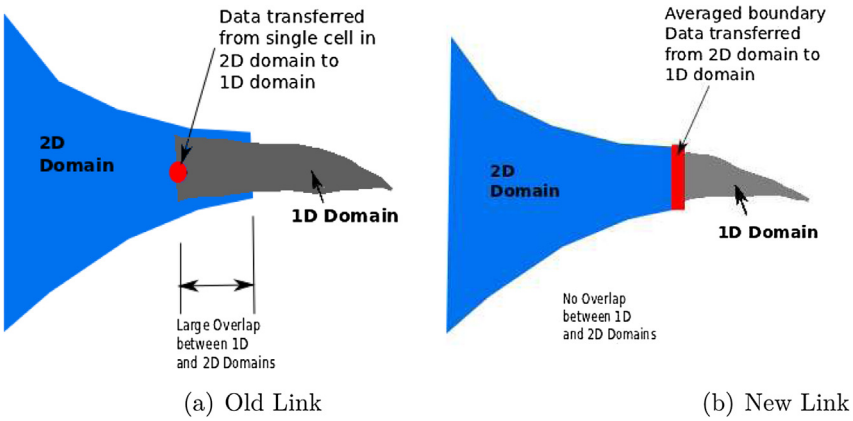

Fig. 7. Changes in 2D-1D linked overlap.

reduction in the MAE value from 0.276 to 0.272 over the three survey points, see Fig. 17 and Table 2), but were important in ensuring that any predictions were consistent with more realistic physical parameters being used over the linked boundary.

3.3.5. Common dispersion coefficients

Likewise, similar results were obtained for the dispersion and diffusion coefficients, where in the old model study the dispersion coefficients in the 2-D model were nearly two orders of magnitude greater than the corresponding values in the 1-D model, at the same location (Milepost 7). A similar comparison again showed that the peak concentration did not match the measured values quite so closely in comparison to the old model (see Fig. 9 and Table 2), but that the lower values were much more closely predicted (with a MAE value of 0.333 overall of the survey points) when an integrated C2C approach was adopted and a unified value of 90 was used for the dispersion constant, k_l, in the dispersion equation (i.e. Equation (8)).

3.3.6. Temperature effects

Primary references addressing water temperature modelling, or concepts related to water temperature modelling, include Fischer et al. (1979), Orlob et al. (1983), Thomann and Mueller (1987) and Chapra (2008). The temperature of the water upstream in the river Ribble was expected to be higher in the bathing season than that of the sea. This is because water from the catchments (i.e. rain water) is generally warmer due to having travelled through warmer air, etc. Also, the wetted area per mass of water is higher in a river as compared to that of the sea. In the previous study by Kashefipour (2002), the same water temperature of 14 °C was used in both the 1-D and 2-D domains of the linked model. The event being modelled took place in June 1999, when the river temperatures were generally higher during this period as compared to the rest of the year. Furthermore, the river was generally warmer upstream as compared to downstream. To evaluate the effects of a higher temperature in the 1-D part of the dynamically linked model, a revised model was set up with a water temperature of 18 °C at the upstream boundary of the 1-D model domain. A water temperature of 14 °C was assumed at the downstream boundary of the 2-D model domain. The water temperature was modelled as a solute using a simplified heat balance equation (Edinger and Brady, 1974). An overall heat exchange coefficient of 20.0 W/m^2/°C was assumed, together with an equilibrium temperature of 14 °C. The resulting variation of water temperature in the 2-D domain of the model is shown in Fig. 10.

The resulting faecal coliform levels due to the effects of varying water temperature on decay rates are shown in Fig. 11. The effect of temperature was small (with a MAE value of

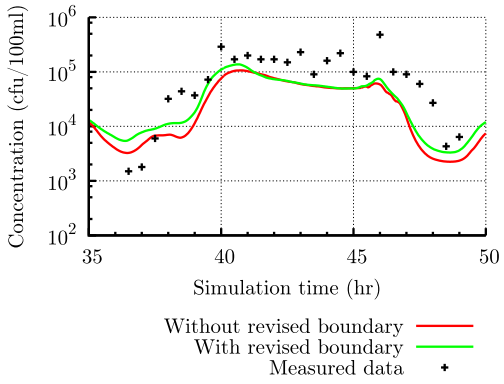

Fig. 8. Comparison of predicted and observed coliform bacteria concentrations at Milepost 7.

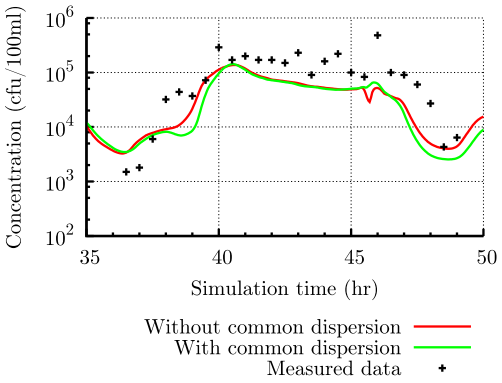

Fig. 9. Faecal coliform concentration levels at Milepost 7.

0.294 over the three survey points as shown in Table 2 and Fig. 17), but this impact was important in accurately determining the peak concentrations.

3.3.7. Salinity effects

It is known that when the salinity of water is high the decay rate for coliform is increased. According to Mancini (1978), as the salinity of the water increases the mortality rate (decay rate) of coliform bacteria also increases and this relationship is linear. In this section, modelling the effect of salinity on the decay rates for faecal coliform is described.

The salinities of fresh water and seawater were assumed to be 0.5 ppt (parts per thousand) and 35 ppt respectively. The salinity of seawater around the U.K. is known to range from about 31 ppt to 38 ppt. The 2-D domain of the dynamically linked model was set up with the seawater salinity as a constant solute concentration (i.e. no change with time) at the north, south and western boundaries. At the upstream boundaries for the 1-D domain of the model, the salinity concentration was set as a constant value equal to the assumed fresh water salinity.

Modelling the salinity as a solute with a zero decay rate (i.e. a conservative tracer) gave a tidal variation of salinity at the mouth of the estuary as shown in Fig. 12.

The effect of salinity was then linked to the decay rate of the bacteria (see Equations (9) and (11)). The overall effective decay rates were increased during the day and night time due to salinity effects, as shown in Fig. 13(a). It was noted that increased decay rates occurred with incoming tides and only affected faecal coliform levels that had already made their way downstream and were being brought back upstream by the tides.

The resulting faecal coliform concentrations at the survey points were not greatly affected, with a MAE value of 0.270

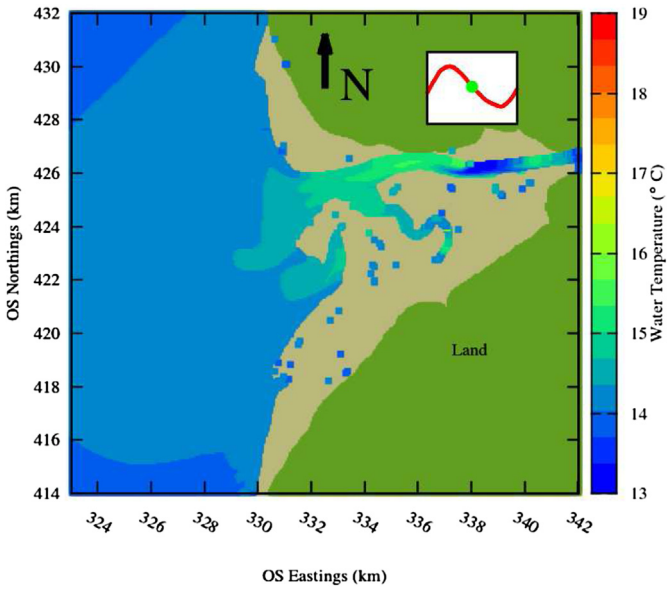

Fig. 10. Variation of water temperature in 2-D domain of model during ebb tide.

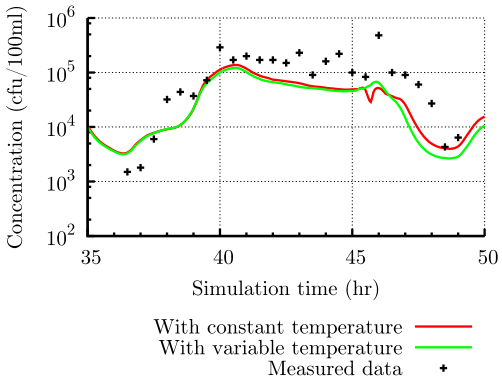

Fig. 11. Coliform concentrations due to water temperature variation at Milepost 7.

(see Table 2 and Fig. 17) over the three survey points as shown in Fig. 13(b) for Milepost 7. However, it was noted that there was a slight influence on the low concentrations.

3.3.8. Solar irradiation effects

Solar irradiation can have a significant effect on decay rates (Kay et al., 2005a), and it is therefore important that its variation in any model provides a good representation of real world conditions. Previous models have often adopted two values for the decay rate, one for day-time and another for night-time conditions. For example Kashefipour et al. (2006) adopted this approach for Irvine Bay in Scotland. In the old linked model, the length of daytime, i.e. from sunrise to sunset was set to 12 h and the full day light decay rate was applied immediately at sunrise and stayed constant until sunset, when it was instantly reverted to the default night-time decay rate. However, the change from total darkness to full day light does not occur instantly in practice and therefore the variation of light on the coliform kinetic processes in the model needed to be refined. Both the duration and intensity of sunshine or solar irradiation varies during the day and during the year, according to Burgess (2009), with this variation being generally approximated by a sinusoidal function.

A revised model was therefore set up using a sinusoidal function to represent how the light intensity varied during the day. The effect of solar irradiation was modelled using Equation (10), as given by Thomann and Mueller (1987), without considering the effect of turbidity in the form of light extinction over the depth of the water column. The resulting variation of the effective decay rates are shown in Fig. 14(a).

The results illustrated in Fig. 14(b) show that the effects of a sinusoidal variation of day light intensity led to a slightly higher peak concentration. It was also noted that even though the effects were small (with a MAE value of 0.236 over the three survey points), they contributed to more accurate coliform concentration predictions than the effects of water temperature (with a MAE of 0.294) and salinity (with a MAE value of 0.270) as shown in Table 2 and Fig. 17.

3.3.9. Turbidity

The effects of solar irradiation on decay rates are further influenced by the ability of light to travel through the water

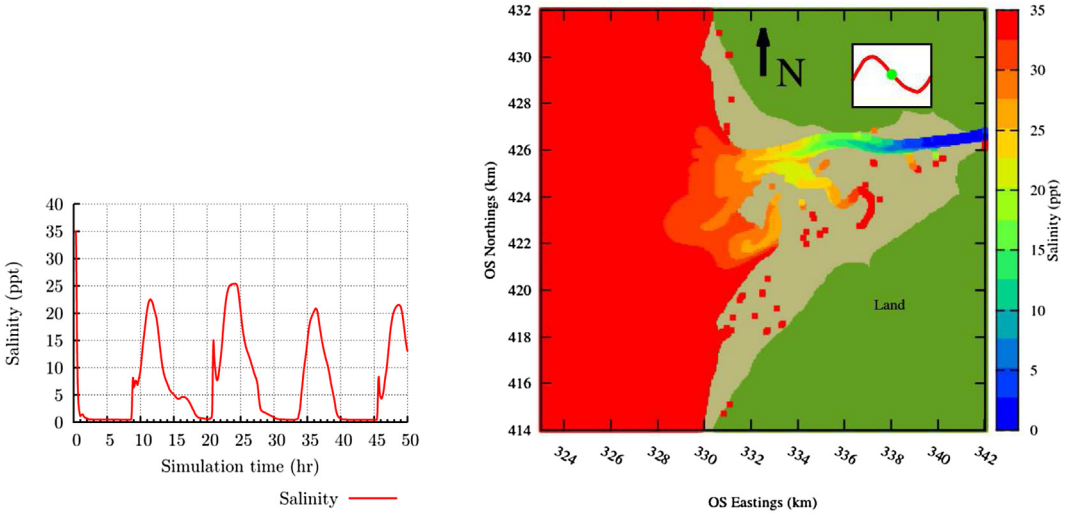

(a) Variation with time at Milepost 7 (b) Variation with position during ebb tide

Fig. 12. Variation of salinity in Ribble Estuary.

column. The presence of water itself attenuates or reduces the distance travelled by the incident solar irradiation. In addition to this process, the presence of any particulate matter in the water column further reduces this distance. According to Burton et al. (1995), observations of the Ribble revealed the existence of a turbidity maximum between the head of the estuary at Penwortham and the Ribble/Douglas confluence. Recent observations of the Ribble Basin have confirmed that the effects of turbidity are also expected to be important. The effect of turbidity was taken into account by introducing a light extinction coefficient, k_e, with a value of 2.37 m^{-1}. The effect of the light extinction co-efficient on the effective decay rate at Milepost 7 is shown in Fig. 15(a), with the overall MAE value of 0.196 over the three survey points being less than the values obtained for the previous environmental factors considered (as shown in Table 2 and Fig. 17). The peak decay rates have been reduced. This effect is much less pronounced where the water depth is low.

3.3.10. Combined effects

A revised model was then set up to combine all of the various factors discussed in the previous sections of this paper. The resulting faecal coliform levels are shown in Fig. 16(b). In comparing the total effective decay rates of the integrated model to those of the old model, it was observed that there were higher decay rates during the daytime hours (Fig. 16(a)). The peak daytime decay rates could be further reduced if cloud cover was considered. Cloud cover could explain why the expected decay rates for daytime irradiation levels were not being achieved. Variability of cloud cover could also help quantify the sensitivity of bacterial counts when making water quality management decisions based on deterministic models. Also, the low peak coliform levels (Fig. 16(b)), could be due to the possibility that not all of the agricultural and urban run-off inputs had been included in the model.

A comparison of the overall effects of a more integrated C2C approach to the Ribble estuary was carried out (Fig. 17).

A comparison of the differing parameter scenarios in Fig. 17 shows that the combined model had a lower MAE value of 0.203. The mean absolute error (MAE) was calculated for the $\log_{10}$ transformed solute concentrations over three survey points (Milepost 7, Milepost 3 and Bullnose). According to Stapleton et al. (2008), the distribution of $\log_{10}$ transformed faecal indicator concentrations showed a closer

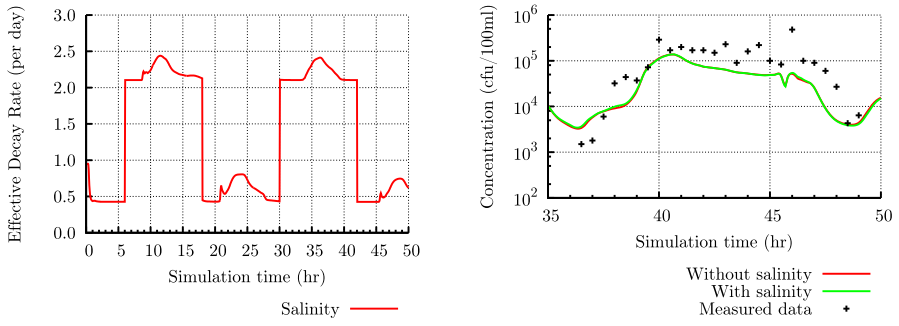

(a) Variation of effective decay rates (k_b') (b) Variation of faecal coliform concentration levels

Fig. 13. Effects of salinity at Milepost 7.

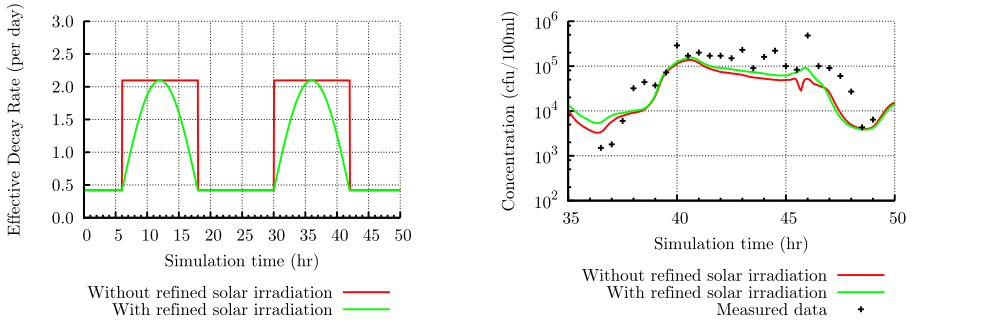

(a) Variation of effective decay rates (k_b') (b) Variation of faecal coliform concentration levels

Fig. 14. Effects of solar irradiation at Milepost 7.

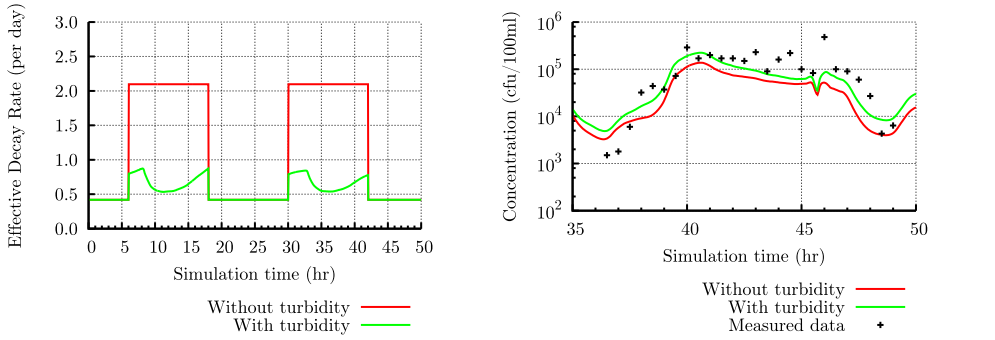

(a) Variation of effective decay rates (k_b') (b) Variation of faecal coliform concentration levels

Fig. 15. Effects of turbidity at Milepost 7.

approximation to a normal probability density function and hence is more suitable for statistical analysis. The introduction of a common decay rate had a negative impact on the predicted coliform levels. However, this is due to the removal of factors which may affect the river upstream differently to the wider estuary downstream. The effects of solar radiation and turbidity had a greater positive impact on the predicted coliform levels. Therefore the accuracy of the solar radiation and turbidity parameters are important for the Ribble estuary. Better or more data on solar radiation and turbidity would help to improve on the ability to predict the quality of the bathing waters. In this research study, a single light extinction coefficient was applied to the estuary. Further refinement of this parameter, including spatial and temporal variation linked representation to the suspended sediment transport concentrations, may help further in improving the performance of future models.

4. Conclusions

The paper has revisited a previous modelling study of the Ribble Basin. Many of the deficiencies in the traditional approach relate to the modelling studies not being fully integrated, and with each different model domain being calibrated

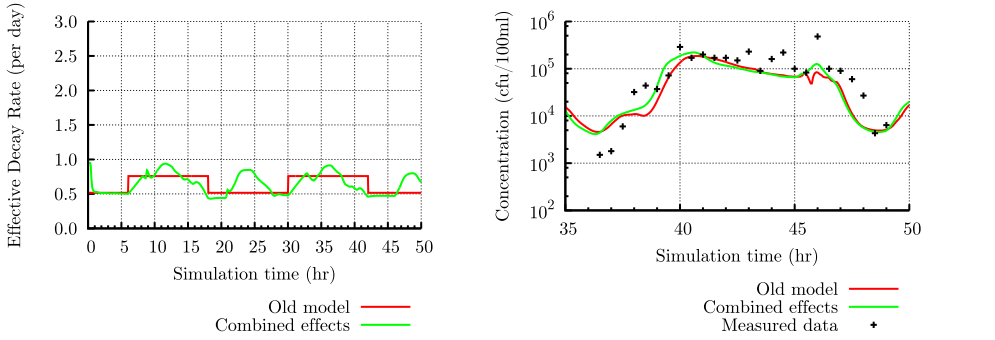

(a) Variation of effective decay rates (k_b') (b) Variation of faecal coliform concentration levels

Fig. 16. Integrated new model at Milepost 7.

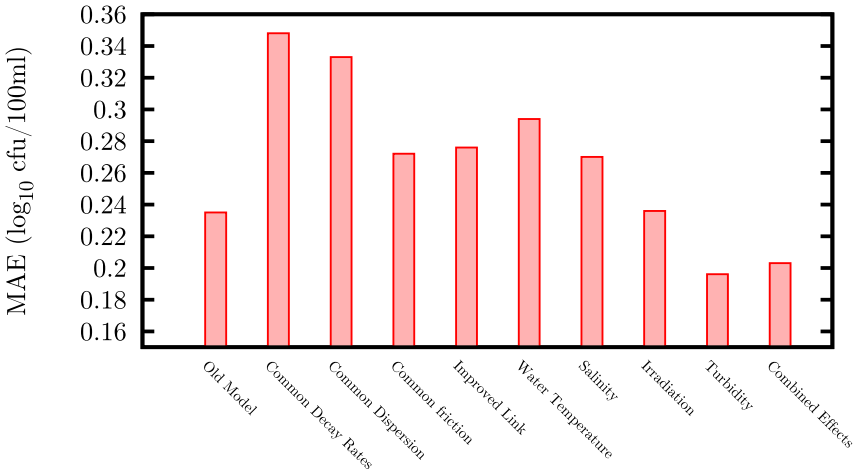

Fig. 17. Comparison of faecal coliform mean absolute error (MAE).

independently. A C2C solutions approach was applied to the Ribble Basin to address these deficiencies by introducing an integrated modelling approach, including: common base decay rates; common bed friction formulations; common dispersion formulations and constants in both the 1-D and 2-D domains of the integrated model. The artificial boundary between the 1-D and 2-D model domains was also improved by removal of the 2.3 km overlap and varying the value of Manning's roughness coefficient gradually at the boundary.

The kinematic representation of bacterial decay was refined by: refining its variation with solar irradiation to be sinusoidal, as opposed to a stepped change from night to day-time; including the effects of turbidity; salinity and temperature variation within the Ribble Basin. The sinusoidal representation of sunlight intensity was found to be more representative of the change in solar radiation, in comparison with a step-wise change.

The new model approach developed herein represents the underlying fluid mechanics better, predicts coliform levels that will not change significantly if the location of the 1-D/2-D model boundary is moved and has a more refined bio-kinetic representation. This is important for real time bathing water quality predictions.

A comparison of the C2C approach to modelling has shown that this approach results in a better representation of the fluid mechanics, particularly at model boundaries, and leads to more robust and accurate results. Therefore better decisions can be made when considering investment strategies appropriate for various treatment options and solutions in the river basin upstream. This is becoming increasingly important with the need to determine accurately the relationship between faecal indicator organism (FIO) sources and failure to comply with the EU mandatory water quality standards of the Bathing Water Framework Directive. There is also a need for tools that can provide rapid forecasting of the likely FIO concentrations. A C2C approach together with a refined bio-kinetic representation in models, can therefore be used in the future development of these rapid assessment tools for strategic water management.

Acknowledgements

The lead author would like to thank the Natural Environment Research Council (NERC) and CH2M Hill (previously Halcrow) who have funded the Industrial Open Case Studentship (Grant Number NE/H018131/1), through which this research work was carried out.

References

Boye, B.A., Falconer, R.A., Akande, K., 2013. Integrated water management solutions from cloud to coast: application to Ribble Basin. In: Proceedings of the 35th IAHR World Congress, vol. 4.1. IAHR, Chengdu, China, pp. 1–12.

Burgess, P., 2009. Variation in Light Intensity at Different Latitudes and Seasons, Effects of Cloud Cover and the Amounts of Direct and Diffused Light. www.ccfg.org.uk/conferences/downloads/P_Burgess.pdf. Presentation to Continuous Cover Forestry Group (CCFG) Scientific Meeting [Online; accessed July-2012].

Burton, D.J., West, J.R., Horsington, R.W., Randle, K., 1995. Modelling transport processes in the Ribble estuary. Environ. Int. 21 (2), 131–141.

Chan, S., Thoe, W., Lee, J., 2013. Real-time forecasting of Hong Kong beach water quality by 3D deterministic model. Water Res. 47 (4), 1631–1647.

Chapra, S.C., 2008. Surface Water-quality Modeling. Waveland Press, Incorporated, p. 844.

Crowther, J., Kay, D., Wyer, M.D., 2001. Relationships between microbial water quality and environmental conditions in coastal recreational waters: the Fylde Coast, UK. Water Res. 35 (17), 4029–4038.

Edinger, J.E., Brady, D.K., 1974. Heat Exchange and Transport in the Environment, vol. 14. John Hopkins University, Electric Power Research Institute, Palo Alto, California, p. 125.

Elder, J.W., 1959. The dispersion of marked fluid in turbulent shear flow. J. Fluid Mech. 5 (04), 544–560.

European Parliament, C, 2006. Directive 2006/7/EC of the European Parliament and of the Council of 15 February 2006 concerning the management of bathing water quality and repealing directive 76/160/EEC. J. Eur. Union 15. European Parliament, Council.

Falconer, R.A., Chen, Y., 1996. Modelling sediment transport and water quality processes on tidal floodplains. In: Anderson, M.G., Walling, D.E., Bates, P.D. (Eds.), Floodplain Processes. John Wiley and Sons, Ltd, pp. 361–398 (chapter 11).

Fischer, H.B., List, E.J., Koh, R.C.Y., Imberger, J., Brooks, N.H., 1979. Mixing in Inland and Coastal Waters. Academic Press Inc, San Diego, p. 483.

Kashefipour, S., 2002. Modelling Flow, Water Quality and Sediment Transport Processes in Riverine Basins. Ph.D. thesis. Cardiff University, UK.

Kashefipour, S.M., Falconer, R.A., 2002. Longitudinal dispersion coefficients in natural channels. Water Res. 36 (6), 1596–1608.

Kashefipour, S., Lin, B., Falconer, R.A., 2005. Neural networks for predicting seawater bacterial levels. Proc. Inst. Civ. Eng. Water Manag. 158 (3), 111–118.

Kashefipour, S.M., Lin, B., Falconer, R.A., 2006. Modelling the fate of faecal indicators in a coastal basin. Water Res. 40 (7), 1413–1425.

Kashefipour, S., Lin, B., Harris, E., Falconer, R.A., 2002. Hydro-environmental modelling for bathing water compliance of an estuarine basin. Water Res. 36 (7), 1854–1868.

Kay, D., Crowther, J., Fewtrell, L., Francis, C., Hopkins, M., Kay, C., McDonald, A., Stapleton, C., Watkins, J., Wilkinson, J., Wyer, M., 2008. Quantification and control of microbial pollution from agriculture: a new policy challenge? Environ. Sci. Policy 11 (2), 171–184.

Kay, D., Jones, F., Wyer, M., Fleisher, J., Salmon, R., Godfree, A., Zelenauch-Jacquotte, A., Shore, R., 1994. Predicting likelihood of gastroenteritis from sea bathing: results from randomised exposure. Lancet 344 (8927), 905–909.

Kay, D., Stapleton, C., Wyer, M., McDonald, A., Crowther, J., Paul, N., Jones, K., Francis, C., Watkins, J., Wilkinson, J., Humphrey, N., Lin, B., Yang, L., Falconer, R., Gardner, S., 2005a. Decay of intestinal enterococci concentrations in high-energy estuarine and coastal waters: towards real-time T90 values for modelling faecal indicators in recreational waters. Water Res. 39 (4), 655–667.

Kay, D., Wyer, M., Crowther, J., Stapleton, C., Bradford, M., McDonald, A., Greaves, J., Francis, C., Watkins, J., 2005b. Predicting faecal indicator fluxes using digital land use data in the UK's sentinel water framework directive catchment: the Ribble study. Water Res. 39 (16), 3967–3981.

Lyons, M., 1997. The dynamics of suspended sediment transport in the Ribble estuary. Water Air Soil Pollut. 99 (1–4), 141–148.

Mancini, J.L., 1978. Numerical estimates of coliform mortality rates under various conditions. Water Pollut. Control Fed. 50 (11), 2477–2484.

Mansilha, C.R., Coelho, C.A., Heitor, A.M., Amado, J., Martins, J.P., Gameiro, P., 2009. Bathing waters: new directive, new standards, new quality approach. Mar. Pollut. Bull. 58 (10), 1562–1565.

Nicholis, G., 2006. Infection risks from water in natural and man-made environments. Eurosurveillance 11, 76–78.

Orlob, G.T., Jorgensen, S.E., Beck, M.B., Loucks, D.P., Gromiec, M.J., Mauersberger, P., Harleman, D.R.F., Vasiliev, O.F., Jacquet, J., Watanabe, M., 1983. Mathematical Modeling of Water Quality: Streams, Lakes, and Reservoirs, illustrated edition. In: International Series on Applied Systems Analysis. Wiley, p. 518.

Pond, K., 2005. Water Recreation and Disease: Plausibility of Associated Infections: Acute Effects, Sequelae, and Mortality, illustrated edition. In: Emerging Issues in Water and Infectious Disease Series. World Health Organization, p. 239.

Preston, R.W., 1985. The Representation of Dispersion in Two-dimensional Shallow Water Flow. CEGB Report No. TPRD/L/2783/N84. Central Electricty Research Laboratories, p. 13.

Prüss, A., 1998. Review of epidemiological studies on health effects from exposure to recreational water. Int. J. Epidemiol. 27 (1), 1–9.

Schets, F.M., Schijven, J.F., de Roda Husman, A.M., 2011. Exposure assessment for swimmers in bathing waters and swimming pools. Water Res. 45 (7), 2392–2400.

Stapleton, C., Wyer, M., Crowther, J., McDonald, A., Kay, D., Greaves, J., Wither, A., Watkins, J., Francis, C., Humphrey, N., Bradford, M., 2008. Quantitative catchment profiling to apportion faecal indicator organism budgets for the Ribble system, the UK's sentinel drainage basin for water framework directive research. J. Environ. Manag. 87 (4), 535–550.

The Royal Academy of Engineering, 2010. Global Water Security: an Engineering Perspective. http://www.raeng.org.uk/news/publications/list/reports/Global_Water_Security_report.pdf [Online; accessed July-2011].

Thoe, W., Wong, S., Choi, K., Lee, J., 2012. Daily prediction of marine beach water quality in Hong Kong. J. Hydro Environ. Res. 6 (3), 164–180.

Thomann, R., Mueller, J., 1987. Principles of Surface Water Quality Modeling and Control. Harper Collins Publishers Inc, p. 644.

United Utilities, 2013. Enhancing Preston's Sewer System. http://www.unitedutilities.com/Preston.aspx [Online; accessed June-2013].

Wu, W., 2008. Computational River Dynamics. Taylor & Francis, p. 494.

Zhou, J., Falconer, R.A., Lin, B., 2014. Refinements to the {EFDC} model for predicting the hydro-environmental impacts of a barrage across the Severn Estuary. Renew. Energy 62 (0), 490–505.